



OPEN ACCESS

EDITED BY
Dangpeng Xi,
China University of Geosciences, China

REVIEWED BY
Mao Luo,
Nanjing Institute of Geology and
Paleontology (CAS), China

*CORRESPONDENCE
Jing Lu
✉ lujing@cumtb.edu.cn

RECEIVED 28 August 2023
ACCEPTED 06 October 2023
PUBLISHED 18 October 2023

CITATION
Zhang P, Yang M, Jiang Z, Zhou K, Xu X,
Chen H, Zhu X, Guo Y, Ye H, Zhang Y,
Shao L and Lu J (2023) Significant floral
changes across the Permian-Triassic
and Triassic-Jurassic transitions
induced by widespread wildfires.
Front. Ecol. Evol. 11:1284482.
doi: 10.3389/fevo.2023.1284482

COPYRIGHT
© 2023 Zhang, Yang, Jiang, Zhou, Xu, Chen,
Zhu, Guo, Ye, Zhang, Shao and Lu. This is an
open-access article distributed under the
terms of the [Creative Commons Attribution
License \(CC BY\)](https://creativecommons.org/licenses/by/4.0/). The use, distribution or
reproduction in other forums is permitted,
provided the original author(s) and the
copyright owner(s) are credited and that
the original publication in this journal is
cited, in accordance with accepted
academic practice. No use, distribution or
reproduction is permitted which does not
comply with these terms.

Significant floral changes across the Permian-Triassic and Triassic-Jurassic transitions induced by widespread wildfires

Peixin Zhang^{1,2}, Minfang Yang³, Zhongfeng Jiang¹, Kai Zhou⁴,
Xiaotao Xu⁵, Huijuan Chen¹, Xuran Zhu¹, Yanghang Guo¹,
Huajun Ye¹, Yuchan Zhang¹, Longyi Shao² and Jing Lu^{2*}

¹School of Municipal and Environmental Engineering, Henan University of Urban Construction, Pingdingshan, Henan, China, ²State Key Laboratory of Coal Resources and Safe Mining, College of Geoscience and Surveying Engineering, China University of Mining and Technology, Beijing, China, ³Research Institute of Petroleum Exploration and Development, PetroChina, Beijing, China, ⁴State Key Laboratory of Hydroscience and Engineering, Department of Hydraulic Engineering, Tsinghua University, Beijing, China, ⁵General Prospecting Institute of China National Administration of Coal Geology, Beijing, China

Wildfires are a major source of perturbations to the Earth's system and have important implications for understanding long-term interactions between the global environment, climate, and organisms. In this study, current evidence for global warming, wildfires, and floral changes across the Permian-Triassic (P-T) and Triassic-Jurassic (T-J) transitions were reviewed, and their relationships were discussed. Available evidence suggests that global plant community turnover and the decline in plant diversity across the P-T and T-J boundaries were primarily driven by widespread wildfires. The Siberian Large Igneous Province and Central Atlantic Magmatic Province released large amounts of isotopically light CO₂ into the atmospheric system, contributing to global warming and increased lightning activity. This ultimately led to an increase in the frequency and destructiveness of wildfires, which have significantly contributed to the deterioration of terrestrial ecosystems, the turnover of plant communities, and the decline in plant diversity. Furthermore, frequent wildfires also constitute an important link between land and ocean/lake crises. Large amounts of organic matter particles and nutrients from the weathering of bedrock after wildfires are transported to marine/lake systems through runoff, contributing to the eutrophication of surface water and the disappearance of aerobic organisms, as well as hindering the recovery of aquatic ecosystems. These wildfire feedback mechanisms provide an important reference point for environmental and climatic changes in the context of current global warming. Therefore, the interplay between global warming, wildfires, and biological changes and their feedback mechanisms needs to be fully considered when assessing current and future risks to the Earth's surface systems.

KEYWORDS

Permian-Triassic transition, Triassic-Jurassic transition, global warming, widespread wildfires, floral change

1 Introduction

Increased global warming, a trend that has been a result of human activity since the mid-20th century, has already led to an increase in the frequency and severity of fire weather worldwide, increasing the risk of wildfires (Jones et al., 2020; Sharifi, 2022). Previous studies have shown that climate change will increase the risk of wildfires, with a global increase in average temperatures; frequency and intensity/extent of heatwaves, and regional increases in the duration, intensity and frequency of droughts, have the potential to influence fire weather, and thus increase the ignition potential of wildfires (Jones et al., 2020; Sharifi, 2022). The potential of wildfire occurrence is increasing at an unprecedented rate, possibly comparable to the rapid climatic changes affecting Earth's ecosystems in its geological past.

Widespread wildfires have played an important role in the Earth's system changes since the emergence of Silurian land plants, profoundly affecting the patterns and processes of global ecosystems (e.g., Glasspool, 2000; Scott, 2000; Glasspool et al., 2004; Glasspool et al., 2015; Lu et al., 2020; Glasspool and Gastaldo, 2022;

Xu et al., 2022; Zhang et al., 2022; Zhang et al., 2023a). Changes in wildfire activity in Earth's history can be identified in sediment records through variations in the by-products of plant combustion, such as charcoal fossils, fusinite, and polycyclic aromatic hydrocarbons (PAHs) (e.g., Glasspool, 2000; Glasspool et al., 2004; Shen et al., 2011; Glasspool et al., 2015; Lu et al., 2020; Song et al., 2020; Glasspool and Gastaldo, 2022; Song et al., 2022; Xu et al., 2022; Zhang et al., 2022; Jiao et al., 2023; Zhang et al., 2023a). The earliest wildfires (inferred from charcoal fossils) date back to the Silurian period (*ca.* 400 Ma) (Glasspool et al., 2004) and are consistent with the first records of terrestrial flora (Belcher and Claire, 2013). Therefore, the record of wildfire activity extends throughout Earth's turbulent climate history, covering many large and small timespans of climate changes over geologic periods that have been accompanied by global fluctuations in O₂, CO₂, and temperature (Figures 1A–C), including four of the 'Big Five' mass extinctions (Figures 1D–F).

The Permian-Triassic (P-T) and the Triassic-Jurassic (T-J) mass extinctions, the first and third largest biotic crises in the Phanerozoic, respectively (e.g., Alroy, 2014; Dal Corso et al.,

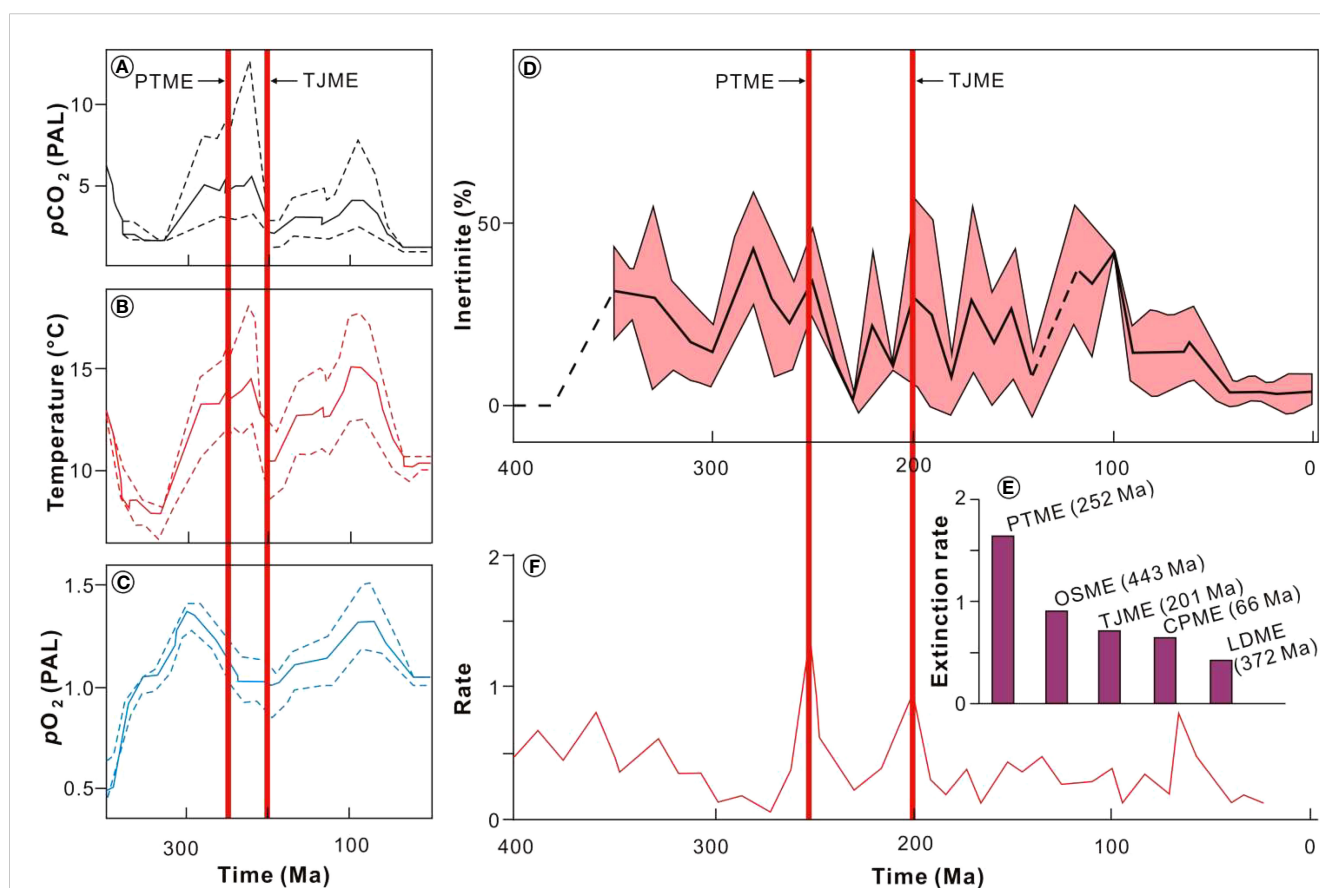


FIGURE 1

Global warming/climatic disturbance event occurrences and their relationship to: (A) Modelled atmospheric CO₂ concentrations; (B) Modelled average global temperatures; (C) Modelled atmospheric oxygen concentrations (with uncertainty range (dotted line)) (modified from Lenton et al., 2018); (D) Inertinite abundance (bin mean) from fossil peat deposits (modified from Glasspool and Scott, 2010); (E, F) Macro-evolutionary rates of extinction of fossil marine invertebrate taxa, from the Paleobiology Database (modified from Blois et al., 2013 and Dal Corso et al., 2022). PAL, present atmospheric level; PTME, Permian-Triassic mass extinction; TJME, Triassic-Jurassic mass extinction; OSME, Ordovician-Silurian mass extinction; CPME, Cretaceous-Paleogene mass extinction; LOME, Late Devonian mass extinction.

2022), were accompanied by significant changes in global atmospheric composition, environment, climate, and flora (Shen et al., 2019; Wignall and Atkinson, 2020; Dal Corso et al., 2022; Shen et al., 2022b; Shen et al., 2023). Available evidence suggests that the mass extinction of terrestrial and marine life during these events were ultimately caused by the eruptions of the Siberian Large Igneous Province (SLIP) and Central Atlantic Magmatic Province (CAMP) (Wignall and Atkinson, 2020; Dal Corso et al., 2022), which was accompanied by a combination of massive releases of greenhouse gases and toxic gases (Fielding et al., 2019; Cui et al., 2021; Shen et al., 2022a; Zhang et al., 2022; Wu et al., 2023), rapid global warming (McElwain et al., 1999; Bonis et al., 2010; Schaller et al., 2011; Sun et al., 2012; Wu et al., 2021), negative carbon isotope excursions (CIEs) (Hesselbo et al., 2002; Shen et al., 2011; Kovács et al., 2020; Ruhl et al., 2020; Wu et al., 2020; Shen et al., 2022b), widespread wildfires (Belcher et al., 2010; Shen et al., 2011; Petersen and Lindström, 2012; Lu et al., 2020; Song et al., 2020; Song et al., 2022; Jiao et al., 2023), increased continental weathering (Cao et al., 2019; Lu et al., 2020; Shen et al., 2022b), and increased erosion (Biswas et al., 2020; van de Schootbrugge et al., 2020; Kaiho et al., 2021).

In this study, published records of terrestrial wildfires and floral changes across the P-T and T-J transitions were reviewed to assess potential relationships between SLIP and CAMP eruptions, global warming, wildfires, and floral extinction/turnover. This will provide deeper insight into the effects of contemporary environmental changes and the response mechanisms of the Earth's ecosystems to these changes.

2 Floral changes across the Permian-Triassic transition

During the P-T transition interval, rapid extinctions/disappearances of terrestrial plant communities and catastrophic declines in plant diversity occurred across different geographic and climatic zones (e.g., Fielding et al., 2019; Chu et al., 2020; Feng et al., 2020; Gastaldo et al., 2020; Mays et al., 2020; Shu et al., 2022; Shao et al., 2023). This redefined the history of floral evolution, followed by the Early-Middle Triassic coal gap (the interval between the disappearance of coal-forming plants). Global coal-forming plants did not fully recover and form global coal deposits until the Late Triassic Carnian (e.g., Gastaldo et al., 1996; Dal Corso et al., 2020; Zhang et al., 2023b). Although some studies suggest that terrestrial plant loss was relatively milder compared to that of animals (Schneebeil-Hermann et al., 2017; Nowak et al., 2019), the abrupt halt in global peat formation represents a clear signal of significant terrestrial plant loss during the P-T transition (Gastaldo et al., 1996; Dal Corso et al., 2020).

In the high latitudes of the Southern Hemisphere, plant macro- and microfossils in Australia indicate the rapid transformation of *Glossopteris* flora into gymnosperms (lycopodium) and fern dominated flora during the P-T transition interval, and the subsequent loss of coal seam and rapid colonization of planktonic algae, fungi, and bacteria (Fielding et al., 2019; Mays et al., 2020;

Vajda et al., 2020; Mays et al., 2021; McLoughlin et al., 2021). In the mid-latitudes of the Southern Hemisphere, plant communities from the Karoo Basin (inferred from plant macro- and microfossils) have undergone similar transformations, characterized by taeniate bisaccate *Protohaploxylinus* and *Striatopodocarpidites* pollen are replaced by assemblages rich in algal remains and low abundance of non-taeniate, aleate bisaccate pollen and cavate spores (Gastaldo et al., 2020), and the rapid increases followed by rapid decreases trend in the terrestrial plant index (the ratios of normal alkanes of terrestrial plant origin to total normal alkanes) from Guryul Ravine, India, indicates that the land plant community has also experienced catastrophic losses, characterized by a sharp reduction in the amount of terrestrial vegetation, occurred before and at the end-Permian marine extinction (Aftabuzzaman et al., 2021).

Near the equator, plant macrofossil records in South China show that terrestrial plants across the P-T transition led to the rapid disappearance of coal-forming plants such as lycopodium, ferns, seed ferns, and cycads in Cathaysia flora, with species reduction of 95% and genera reduction of 50% (Zhang et al., 2016; Chu et al., 2020; Feng et al., 2020). The latest palynological fossil results show the occurrence of two significant changes in the terrestrial plant community and plant diversity in South China across the P-T transition (Hua et al., 2023; Shao et al., 2023). The first was accompanied by a significant change of plant community dominated by *Gigantopteris* to gymnosperms, and the second was accompanied by a collapse of plant community and a significant decline in plant diversity (inferred from the disappearance of spores and pollen) (Hua et al., 2023; Shao et al., 2023). In addition, the change trends of land plant indices from South China (including Meishan, Shangsi, Liangfengya, Huangzhishan, and Xiaohebian sections) and Italy (Bulla Section) also show a catastrophic loss of land plant communities across the P-T transition (Biswas et al., 2020; Aftabuzzaman et al., 2021; Kaiho et al., 2021).

In the lower latitudes of the Northern Hemisphere, Cathaysia flora dominated by ferns and *Gigantopteris* gradually disappeared and was transformed into a Euramerican type Zechstein flora dominated by gymnosperms including conifers and pteridosperms (= seed ferns) in the lowest part of the Sunjiagou Formation (Wuchiapingian-Changxingian Stage transition) of the NCP (e.g., Wang and Chen, 2001; Yang and Wang, 2012; Lu et al., 2020). In the middle and/or upper part of the Sunjiagou Formation (Late Permian), plant macrofossil records show the disappearance of approximately 54% (14/26) of genera and approximately 88% (28/32) of species (Chu et al., 2015; Chu et al., 2019) and the interval of plant extinctions during the Early Triassic (Shu et al., 2022). Recent palynological results also indicate a catastrophic loss of terrestrial plant communities and plant diversity in the Yiyang coalfield of the NCP across the P-T transition (Zhang et al., 2023a). In the mid-latitudes of the Northern Hemisphere, the Junggar Basin in northwestern China has also experienced significant terrestrial flora and fauna loss across the P-T transition (Cao et al., 2008; Cai et al., 2021a). In the high latitudes of the Northern Hemisphere, plant macrofossils from Russia show a catastrophic loss of plant communities and plant diversity during this time interval (Krassilov and Karasev,

2009). In summary, the P-T transition experienced a catastrophic loss of terrestrial floras on a global scale.

3 Floral changes across the Triassic-Jurassic transition

During the T-J transition interval, the communities and diversity of terrestrial plants also showed significant changes across different geographic and climatic zones (e.g., Li et al., 2020; Zhang et al., 2022). This reflects another terrestrial plant diversity loss event after a period of complete recovery (the plant radiation during the Carnian Pluvial Episode of the Late Triassic) (Dal Corso et al., 2020; Lu et al., 2021; Zhang et al., 2023b) after the end-Permian terrestrial flora extinctions. This event also had an important impact on the global environment and climate change.

Studies on the western Tethys and Southern Hemisphere report the occurrence of a significant turnover of terrestrial plant communities and a decline in plant diversity across the T-J transition. In the western Tethys (including North America, Germany, Denmark, East Greenland, southwest England, and Austria), floral changes during the T-J transition interval occurred as follows: (1) an end-Triassic fern peak (including *Polypodiisporites polymicroforatus*, and trilete megaspores in some areas); (2) the first appearance of *Cerbropollenites thiergartii* and the last occurrence of *Lunatisporites rhaeticus* during the earliest Jurassic; and (3) a brief proliferation of *Classopollis* pollen (Cheirolepidiaceae) during the earliest Jurassic and the subsequent restoration and dominance of conifers (Olsen et al., 2002; Whiteside et al., 2007; Bonis et al., 2009; van de Schootbrugge et al., 2009; Bonis et al., 2010; Pieńkowski et al., 2012; Vajda et al., 2013; Lindström et al., 2017; Wignall and Atkinson, 2020; Boomer et al., 2021). Similarly, palynological fossil results from New Zealand and Australia in the Southern Hemisphere also show a significant turnover in terrestrial plant

communities (De Jersey and McKellar, 2013). In New Zealand, terrestrial plants from the Late Triassic were dominated by lycophyte and bryophyte spores and crustosperm pollen, and those from the Early Jurassic were dominated by *Osmundaceae* spores and *Classopollis* pollen (Cheirolepidiaceae) (De Jersey and McKellar, 2013). A similar pattern is observed in Australia, where terrestrial plants range from the Late Triassic dominated by ferns and bryophyte spores to the Early Jurassic dominated by Cheirolepidiacean pollen (De Jersey and McKellar, 2013).

Studies on the eastern Tethys also report a significant turnover of terrestrial plant communities and a decline in plant diversity across the T-J transition (Li et al., 2020; Zhou et al., 2021; Shen et al., 2022b; Zhang et al., 2022). In South China, plant macrofossil records (mainly pteridophytes) show a significant turnover of the terrestrial plant community; specifically, drought-resistant plant groups increased significantly across the T-J transition (Zhou et al., 2021). Similarly, palynological fossil results suggest species replacement of the terrestrial plant community, reflected by a change from predominantly pteridophyte lowland vegetation to coniferous species (Li et al., 2020). In North China, palynological fossil records show two significant changes in terrestrial plant communities and a decrease in plant diversity during this time interval (Zhang et al., 2022). In the first instance, the dominant gymnosperm pollen was replaced by algae and fern spores, and the proportion of palynological fossils decreased by ca. 45% (from 38 genera to 21 genera) (Zhang et al., 2022). In the second instance, the dominant fern spores were replaced by gymnosperm pollen, and the proportion of palynological fossils decreased by ca. 44% (from 50 genera to 28 genera) (Zhang et al., 2022). In northwestern China, both plant macro- and microfossils show that the rapid rise of fern spores, and the subsequent change from fern spores to gymnosperms occurred across the T-J transition (Lu and Deng, 2005; Shen et al., 2022b). In summary, terrestrial floras have experienced a significant global turnover of plant communities and a decrease in plant diversity across the T-J transition.

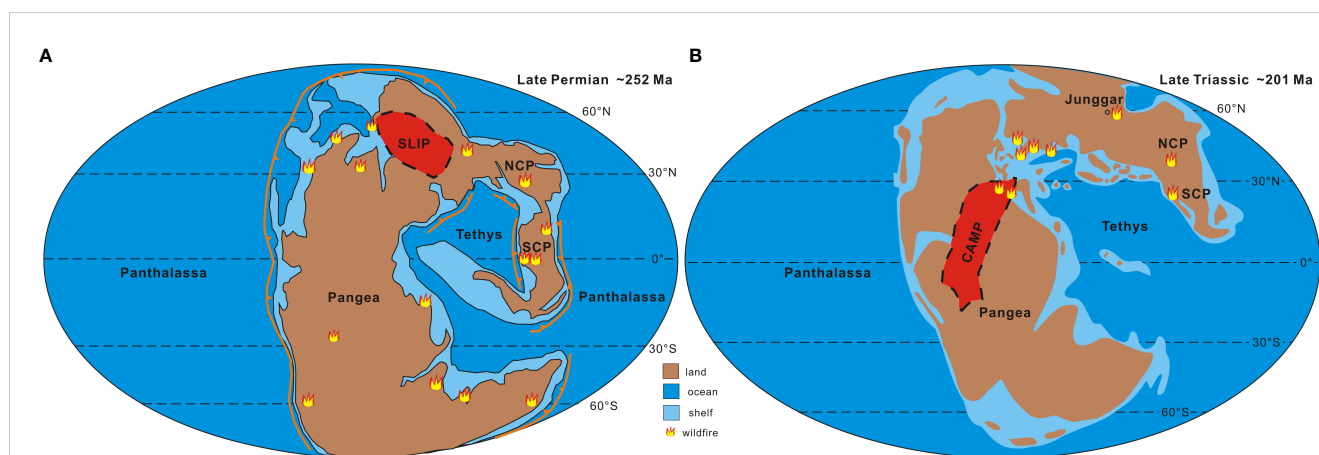
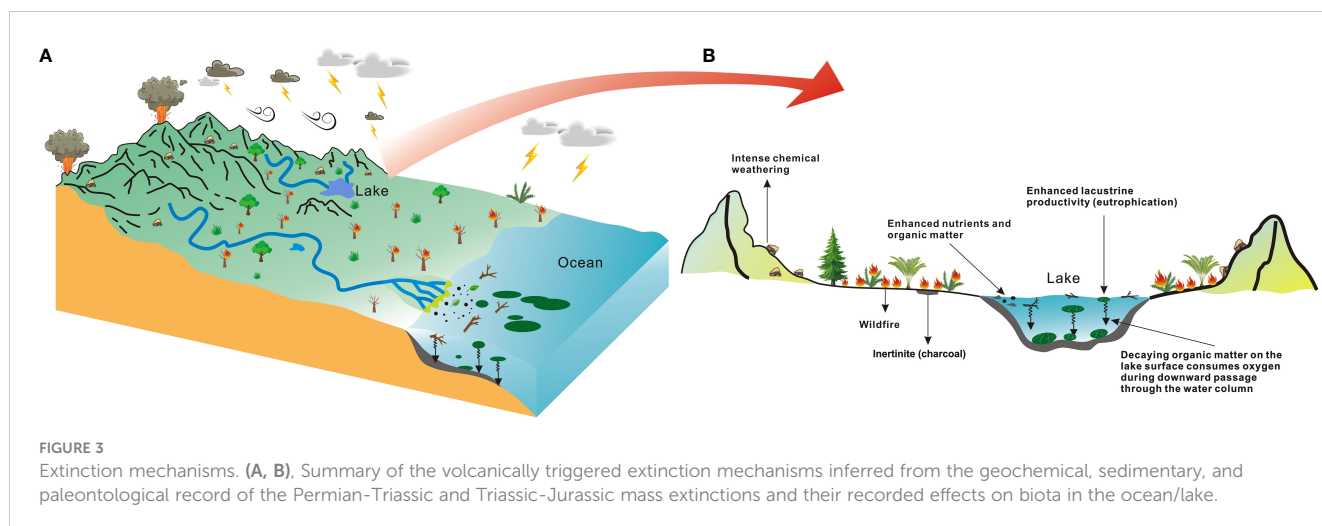


FIGURE 2 Global paleogeography during Permian-Triassic (A) and Triassic-Jurassic (B) transitions, including the location of the Large Igneous Province and wildfires around the world (modified from Lu et al., 2020; Vajda et al., 2020; Zhang et al., 2022; Zhang et al., 2023a). Wildfire distributions from Song et al. (2020), Song et al. (2022), Cai et al. (2021a), and Jiao et al. (2023). NCP, North China Plate; SCP, South China Plate; SLIP, Siberian Large Igneous Province; CAMP, Central Atlantic Magmatic Province.



4 Contemporaneous wildfires linked to volcanism as a potential cause for floral changes

Contemporaneous widespread wildfires are believed to have been a major contributor to changes in the terrestrial environment, climate, and floras across the P-T and T-J transitions (Cao et al., 2008; Shen et al., 2011; Yan et al., 2019; Lu et al., 2020; Cai et al., 2021a; Cai et al., 2021b; Zhang et al., 2022; Zhang et al., 2023a) (Figures 2, 3). During the P-T and T-J transition intervals, published studies have shown that frequent wildfires are primarily controlled by their ignition mechanisms, namely the increased frequency and intensity of lightning activity, which is primarily associated with rapid increases in global temperatures (e.g., Glasspool et al., 2015; Lu et al., 2020; Zhang et al., 2022; Zhang et al., 2023a). Greenhouse warming (increased temperature), related to high CO₂, resulted in an increase of upper-tropospheric water vapor, leading to more lightning activity and storminess (Miller and Baranyi, 2021). During the P-T and T-J transition intervals, SLIP and CAMP released large amounts of isotopically light CO₂ into the atmospheric system, resulting in a significant increase in global temperatures and subsequent enhanced lightning activity (Glasspool et al., 2015; Miller and Baranyi, 2021), ultimately leading to an increase in wildfire frequency and destructiveness (van de Schootbrugge et al., 2008; Belcher et al., 2010; Glasspool et al., 2015; Lu et al., 2020; Zhang et al., 2022; Zhang et al., 2023a) (Figures 2, 3).

Widespread wildfires across the P-T and T-J transitions caused the disappearance/extinction of terrestrial plants, marking significant changes in plant communities and diversity. During the P-T transition interval, evidence from charcoal, fusinite, and PAHs shows the prevalence of massive wildfires worldwide, including eastern Greenland (Nabbefeld et al., 2010), Brazil (Manfroi et al., 2015; Kauffmann et al., 2016), Australia (Glasspool, 2000; Vajda et al., 2020), India (Murthy et al., 2020), Canada (Nabbefeld et al., 2010; Grasby et al., 2011), South China (Shen et al., 2011; Zhang et al., 2016; Yan et al., 2019; Chu et al.,

2020; Cai et al., 2021b; Song et al., 2022; Jiao et al., 2023), North China (Lu et al., 2020; Zhang et al., 2023a), and northwestern China (Cao et al., 2008; Cai et al., 2021a) (Figure 2A). During the T-J transition interval, evidence from charcoal, fusinites, and PAHs shows a global prevalence of large-scale wildfires, including North America (Jones et al., 2002), eastern Greenland (Belcher et al., 2010), Poland (Marynowski and Simoneit, 2009), Denmark (Lindström et al., 2019; Lindström et al., 2021), Sweden (Lindström et al., 2019; Lindström et al., 2021), South China (Pole et al., 2018; Song et al., 2020), and North China (Zhang et al., 2022) (Figure 2B). In addition, frequent wildfires during the aforementioned periods also had positive feedbacks on global warming and the carbon cycle because biomass burning also releases large amounts of isotopically light carbon into the atmosphere, further increasing the magnitude of global warming and CIEs (Ivany and Salawitch, 1993; Belcher et al., 2010).

Frequent wildfires also appear to be an important link between terrestrial and ocean/lake ecological crises. Widespread wildfire damage to surface vegetation can lead to the exposure of bedrock, leading to increased continental weathering, and increased soil erosion (e.g., Glasspool et al., 2015; Lu et al., 2020; Zhang et al., 2022) (Figure 3). These processes can release large amounts of organic matter (including charcoal and un-charred material) and nutrients (including phosphorus and potassium) into the ocean/lake system through surface runoff (Glasspool et al., 2015; Lu et al., 2020; Zhang et al., 2022) (Figure 3). These organic particles temporarily float in the ocean/lake, increasing ocean/lake turbidity through siltation and affecting light penetration and photosynthesis of marine/lake organisms (Glasspool et al., 2015) (Figure 3). Large nutrient inputs to the ocean/lake promote the eutrophication of surface water and the proliferation of cyanobacteria and algae (Liu et al., 2022) (Figure 3). In this context, oxygen circulation between ocean/lake surface water and the atmosphere will be suppressed by floating organic particles, cyanobacteria, and algae (Glasspool et al., 2015). The death of algal blooms reduces the amount of dissolved oxygen in water, produces toxic secondary metabolites (Mays et al., 2021), and enhances alkalinity in local micro-environment via a decaying hydrolytic

destruction (Luo et al., 2021), impeding the recovery of ocean/lake ecosystems (Mays et al., 2021). These combined factors also further contribute to an anoxic environment in the ocean/lake and lead to the extinction of aerobic organisms.

The two examples discussed in this study highlight the interplay between wildfires and a wide range of environmental and climatic change processes in the Earth's surface systems, which is critical to the complete understanding of the feedback effects of wildfires and their changes on terrestrial ecosystems over various time scales. In modern ecosystems, global warming and drought-induced climate conditions triggered by high levels of anthropogenic greenhouse gas emissions pose several risks to the Earth's environment (Sharifi, 2022). In particular, these issues have the potential to increase the probability of widespread natural fires, which have a significant impact on plants, animals, and other natural resources worldwide (Sharifi, 2022). The interaction between fuel and climate and weather conditions determine fire regimes, driving the transformation of smoldering peat fires and low-intensity surface fires to intense crown fires. In turn, these fire regimes influence environmental and climatic change (including atmospheric concentration) over a range of short and long timescales through their feedbacks to geophysical and biological processes. For example, changes in vegetation types can affect wildfire types, and frequent terrestrial wildfires can in turn affect biological and geochemical processes in the Earth's surface systems, such as nutrient transport, resulting in the loss of aerobic organisms in lakes and oceans (Glasspool et al., 2015; Zhang et al., 2022). Similarly, wildfires account for up to 20% of global greenhouse gas production and can travel at speeds of up to 22 km/h, indicating their potential for rapid devastation over large areas of land (Sharifi, 2022). Therefore, when assessing risks to modern and future surface system ecosystems, the interactions and feedback processes between wildfires, climate, and organisms on different time scales should be properly taken into account. An essential requirement for understanding potential future global warming-driven changes in the global fire regime and their impact over time is to clarify these feedback processes and the timescales over which they operate.

5 Conclusion

Studies of wildfires (inferred from charcoal fossils, fusinates, and PAHs) and plants (inferred from macro- and microfossils) across the P-T and T-J transitions have shown that widespread wildfires are the main drivers of the deterioration of terrestrial ecosystems, turnover of plant communities, and decline in plant diversity. SLIP and CAMP can release large amounts of greenhouse gases into the atmospheric system, contributing to global warming and an increase in the frequency of lightning activity, which ultimately enhance the frequency and destructive capacity of wildfires. Wildfires will affect

the global environment through positive feedback effects. In other words, biomass burning will also release large amounts of isotopically light CO₂ into the atmospheric system, further increasing the magnitude of global warming and CIEs. In addition, large amounts of organic particles and nutrients produced by the weathering of bedrock after wildfires are transported to lakes or marine systems through surface runoff, causing eutrophication of surface water and the disappearance of aerobic organisms, as well as hindering the recovery of aquatic ecosystems.

Author contributions

PZ: Writing – review & editing. MY: Writing – review & editing. ZJ: Writing – review & editing. KZ: Writing – review & editing. XX: Writing – review & editing. HC: Writing – review & editing. XZ: Writing – review & editing. YG: Writing – review & editing. HY: Writing – review & editing. YZ: Writing – review & editing, Validation. LS: Writing – review & editing. JL: Writing – original draft, Writing – review & editing.

Funding

The author(s) declare financial support was received for the research, authorship, and/or publication of this article. Financial support was provided by the National Natural Science Foundation of China (42172196, 41772161, and 41472131), the National Key Research and Development Program of China (2021YFC2902000), the Fund of Henan University of Urban Construction (K-Q2023019), and the National Science and Technology Major Project (2017ZX05009-002).

Conflict of interest

Author MY is employed by the company PetroChina and XX is employed by the company China National Administration of Coal Geology.

The remaining authors declare that the research was conducted in the absence of any commercial or financial relationships that could be construed as a potential conflict of interest.

Publisher's note

All claims expressed in this article are solely those of the authors and do not necessarily represent those of their affiliated organizations, or those of the publisher, the editors and the reviewers. Any product that may be evaluated in this article, or claim that may be made by its manufacturer, is not guaranteed or endorsed by the publisher.

References

- Aftabuzzaman, M., Kaiho, K., Biswas, R. K., Liu, Y., Saito, R., Tian, L., et al. (2021). End-Permian terrestrial disturbance followed by the complete plant devastation, and the vegetation proto-recovery in the earliest-Triassic recorded in coastal sea sediments. *Glob. Planet. Change* 205, 103621. doi: 10.1016/j.gloplacha.2021.103621
- Alroy, J. (2014). Accurate and precise estimates of origination and extinction rates. *Paleobiology* 40, 374–397. doi: 10.1666/13036
- Belcher, and Claire, M. (2013). *Fire Phenomena and the Earth System*. Ed. C. M. Belcher (New York: John Wiley & Sons, Ltd). doi: 10.1002/9781118529539
- Belcher, C. M., Mander, L., Rein, G., Jervis, F. X., Haworth, M., Hesselbo, S. P., et al. (2010). Increased fire activity at the Triassic/Jurassic boundary in Greenland due to climate-driven floral change. *Nat. Geosci.* 3, 426–429. doi: 10.1038/ngeo871
- Biswas, R. K., Kaiho, K., Saito, R., Tian, L., and Shi, Z. (2020). Terrestrial ecosystem collapse and soil erosion before the end-Permian marine extinction: Organic geochemical evidence from marine and non-marine records. *Glob. Planet. Change* 195, 103327. doi: 10.1016/j.gloplacha.2020.103327
- Blois, J. L., Zarnetske, P. L., Fitzpatrick, M. C., and Finnegan, S. (2013). Climate change and the past, present, and future of biotic interactions. *Science* 341, 499–504. doi: 10.1126/science.1237184
- Bonis, N. R., Kürschner, W. M., and Krystyn, L. (2009). A detailed palynological study of the Triassic-Jurassic transition in key sections of the Eiberg Basin (Northern Calcareous Alps, Austria). *Rev. Palaeobot. Palynol.* 156, 376–400. doi: 10.1016/j.revpalbo.2009.04.003
- Bonis, N. R., Ruhl, M., and Kürschner, W. M. (2010). Milankovitch-scale palynological turnover across the Triassic-Jurassic transition at St. Audrie's Bay, SW UK. *J. Geol. Soc. London.* 167, 877–888. doi: 10.1144/0016-76492009-141
- Boomer, I., Copestake, P., Raine, R., Azmi, A., Fenton, J. P. G., Page, K. N., et al. (2021). Stratigraphy, palaeoenvironments and geochemistry across the Triassic-Jurassic boundary transition at Carnduff, County Antrim, Northern Ireland. *Proc. Geol. Assoc.* 132, 667–687. doi: 10.1016/j.pgeola.2020.05.004
- Cai, Y., Zhang, H., Cao, C., Zheng, Q., Jin, C., and Shen, S. (2021a). Wildfires and deforestation during the Permian-Triassic transition in the southern Junggar Basin, Northwest China. *Earth-Science Rev.* 218, 103670. doi: 10.1016/j.earscirev.2021.103670
- Cai, Y., Zhang, H., Feng, Z., and Shen, S. (2021b). Intensive wildfire associated with volcanism promoted the vegetation changeover in southwest China during the Permian-Triassic transition. *Front. Earth Sci.* 9. doi: 10.3389/feart.2021.615841
- Cao, C., Wang, W., Liu, L., Shen, S., and Summons, R. E. (2008). Two episodes of ^{13}C -depletion in organic carbon in the latest Permian: Evidence from the terrestrial sequences in northern Xinjiang, China. *Earth Planet. Sci. Lett.* 270, 251–257. doi: 10.1016/j.epsl.2008.03.043
- Cao, Y., Song, H., Algeo, T. J., Chu, D., Du, Y., Tian, L., et al. (2019). Intensified chemical weathering during the Permian-Triassic transition recorded in terrestrial and marine successions. *Palaeogeogr. Palaeoclimatol. Palaeoecol.* 519, 166–177. doi: 10.1016/j.palaeo.2018.06.012
- Chu, D., Grasby, S. E., Song, H. J., Corso, J. D., Wang, Y., Mather, T. A., et al. (2020). Ecological disturbance in tropical peatlands prior to marine Permian-Triassic mass extinction. *Geology* 48, 288–292. doi: 10.1130/G46631.1
- Chu, D., Tong, J., Benton, M. J., Yu, J., and Huang, Y. (2019). Mixed continental-marine biotas following the Permian-Triassic mass extinction in South and North China. *Palaeogeogr. Palaeoclimatol. Palaeoecol.* 519, 95–107. doi: 10.1016/j.palaeo.2017.10.028
- Chu, D., Tong, J., Song, H. J., Benton, M. J., Bottjer, D. J., Song, H. Y., et al. (2015). Early Triassic wrinkle structures on land: Stressed environments and oases for life. *Sci. Rep.* 5, 1–8. doi: 10.1038/srep10109
- Cui, Y., Li, M., Van Soelen, E. E., Peterse, F., and Kürschner, W. M. (2021). Massive and rapid predominantly volcanic CO_2 emission during the end-Permian mass extinction. *Proc. Natl. Acad. Sci. U.S.A.* 118, e2014701118. doi: 10.1073/pnas.2014701118
- Dal Corso, J., Bernardi, M., Sun, Y., Song, H., Seyfullah, L. J., Preto, N., et al. (2020). Extinction and dawn of the modern world in the Carnian (Late Triassic). *Sci. Adv.* 6, eaba0099. doi: 10.1126/sciadv.aba0099
- Dal Corso, J., Song, H., Callegaro, S., Chu, D., Sun, Y., Hilton, J., et al. (2022). Environmental crises at the Permian-Triassic mass extinction. *Nat. Rev. Earth Environ.* 3, 197–214. doi: 10.1038/s43017-021-00259-4
- De Jersey, N. J., and McKellar, J. L. (2013). The palynology of the Triassic-Jurassic transition in southeastern Queensland, Australia, and correlation with New Zealand. *Palynology* 37, 77–114. doi: 10.1080/01916122.2012.718609
- Feng, Z., Wei, H., Guo, Y., He, X., Sui, Q., Zhou, Y., et al. (2020). From rainforest to hermland: New insights into land plant responses to the end-Permian mass extinction. *Earth-Science Rev.* 204, 103153. doi: 10.1016/j.earscirev.2020.103153
- Fielding, C. R., Frank, T. D., McLoughlin, S., Vajda, V., Mays, C., Tevyaw, A. P., et al. (2019). Age and pattern of the southern high-latitude continental end-Permian extinction constrained by multiproxy analysis. *Nat. Commun.* 10, 385. doi: 10.1038/s41467-018-07934-z
- Gastaldo, R. A., DiMichele, W. A., and Pfefferkorn, H. W. (1996). Out of the icehouse into the greenhouse: A late Paleozoic analog for modern global vegetational change. *GSA Today* 6, 1–7.
- Gastaldo, R. A., Kamo, S. L., Neveling, J., Geissman, J. W., Looy, C. V., and Martini, A. M. (2020). The base of the Lystrosaurus Assemblage Zone, Karoo Basin, predates the end-Permian marine extinction. *Nat. Commun.* 11, 1–8. doi: 10.1038/s41467-020-15243-7
- Glasspool, I. (2000). A major fire event recorded in the mesofossils and petrology of the Late Permian, Lower Whybrow coal seam, Sydney Basin, Australia. *Palaeogeogr. Palaeoclimatol. Palaeoecol.* 164, 357–380. doi: 10.1016/S0031-0182(00)00194-2
- Glasspool, I. J., Edwards, D., and Axe, L. (2004). Charcoal in the Silurian as evidence for the earliest wildfire. *Geology* 32, 381. doi: 10.1130/G20363.1
- Glasspool, I. J., and Gastaldo, R. A. (2022). Silurian wildfire proxies and atmospheric oxygen. *Geology* 50, 1048–1052. doi: 10.1130/G50193.1
- Glasspool, I. J., and Scott, A. C. (2010). Phanerozoic concentrations of atmospheric oxygen reconstructed from sedimentary charcoal. *Nat. Geosci.* 3, 627–630. doi: 10.1038/ngeo923
- Glasspool, I. J., Scott, A. C., Waltham, D., Pronina, N., and Shao, L. (2015). The impact of fire on the late Paleozoic Earth System. *Front. Plant Sci.* 6. doi: 10.3389/fpls.2015.00756
- Grasby, S. E., Sanei, H., and Beauchamp, B. (2011). Catastrophic dispersion of coal fly ash into oceans during the latest Permian extinction. *Nat. Geosci.* 4, 104–107. doi: 10.1038/ngeo1069
- Hesselbo, S. P., Robinson, S. A., Surlyk, F., and Piasecki, S. (2002). Terrestrial and marine extinction at the Triassic-Jurassic boundary synchronized with major carbon-cycle perturbation: A link to initiation of massive volcanism? *Geology* 30, 251–254. doi: 10.1130/0091-7613(2002)030<0251:TAMEAT>2.0.CO;2
- Hua, F., Shao, L., Zhang, T., Bond, D. P. G., Wang, X., Wang, J., et al. (2023). An astronomical timescale for the Permian-Triassic mass extinction reveals a two-step, million-year-long terrestrial crisis in South China. *Earth Planet. Sci. Lett.* 605, 118035. doi: 10.1016/j.epsl.2023.118035
- Ivany, L. C., and Salawitch, R. J. (1993). Carbon isotopic evidence for biomass burning at the K-T boundary. *Geology* 21, 487. doi: 10.1130/0091-7613(1993)021<0487:CIEFBB>2.3.CO;2
- Jiao, S., Zhang, H., Cai, Y., Chen, J., Feng, Z., and Shen, S. (2023). Collapse of tropical rainforest ecosystems caused by high-temperature wildfires during the end-Permian mass extinction. *Earth Planet. Sci. Lett.* 614, 118193. doi: 10.1016/j.epsl.2023.118193
- Jones, M. W., Smith, A., Betts, R., Canadell, J. G., Prentice, I. C., and Le Quéré, C. (2020). Climate change increases the risk of wildfires. *Sci. Brief Rev.* 116, 117.
- Jones, T. P., Ash, S., and Figueiral, I. (2002). Late triassic charcoal from petrified forest national park, Arizona, USA. *Palaeogeogr. Palaeoclimatol. Palaeoecol.* 188, 127–139. doi: 10.1016/S0031-0182(02)00549-7
- Kaiho, K., Aftabuzzaman, M., Jones, D. S., and Tian, L. (2021). Pulsed volcanic combustion events coincident with the end-Permian terrestrial disturbance and the following global crisis. *Geology* 49, 289–293. doi: 10.1130/G48022.1
- Kauffmann, M., Jasper, A., Uhl, D., Meneghini, J., Osterkamp, I. C., Zvirtes, G., et al. (2016). Evidence for palaeo-wildfire in the Late Permian palaeotropics—Charcoal from the Motuca Formation in the Parnaíba Basin, Brazil. *Palaeogeogr. Palaeoclimatol. Palaeoecol.* 450, 122–128. doi: 10.1016/j.palaeo.2016.03.005
- Kovács, E. B., Ruhl, M., Demény, A., Fórizs, I., Hegyi, I., Horváth-Kostka, Z. R., et al. (2020). Mercury anomalies and carbon isotope excursions in the western Tethyan Csóvár section support the link between CAMP volcanism and the end-Triassic extinction. *Glob. Planet. Change* 194, 103291. doi: 10.1016/j.gloplacha.2020.103291
- Krassilov, V., and Karasev, E. (2009). Paleofloristic evidence of climate change near and beyond the Permian-Triassic boundary. *Palaeogeogr. Palaeoclimatol. Palaeoecol.* 284, 326–336. doi: 10.1016/j.palaeo.2009.10.012
- Lenton, T. M., Daines, S. J., and Mills, B. J. W. (2018). COPSE reloaded: An improved model of biogeochemical cycling over Phanerozoic time. *Earth-Science Rev.* 178, 1–28. doi: 10.1016/j.earscirev.2017.12.004
- Li, L., Wang, Y., Kürschner, W. M., Ruhl, M., and Vajda, V. (2020). Palaeovegetation and palaeoclimate changes across the Triassic-Jurassic transition in the Sichuan Basin, China. *Palaeogeogr. Palaeoclimatol. Palaeoecol.* 556, 109891. doi: 10.1016/j.palaeo.2020.109891
- Lindström, S., Callegaro, S., Davies, J., Tegner, C., van de Schootbrugge, B., Pedersen, G. K., et al. (2021). Tracing volcanic emissions from the Central Atlantic Magmatic Province in the sedimentary record. *Earth-Science Rev.* 212, 103444. doi: 10.1016/j.earscirev.2020.103444
- Lindström, S., Sanei, H., van de Schootbrugge, B., Pedersen, G. K., Leshner, C. E., Tegner, C., et al. (2019). Volcanic mercury and mutagenesis in land plants during the end-Triassic mass extinction. *Sci. Adv.* 5, eaaw4018. doi: 10.1126/sciadv.aaw4018
- Lindström, S., van de Schootbrugge, B., Hansen, K. H., Pedersen, G. K., Alsen, P., Thibault, N., et al. (2017). A new correlation of Triassic-Jurassic boundary successions in NW Europe, Nevada and Peru, and the Central Atlantic Magmatic Province: A time-line for the end-Triassic mass extinction. *Palaeogeogr. Palaeoclimatol. Palaeoecol.* 478, 80–102. doi: 10.1016/j.palaeo.2016.12.025
- Liu, D., Zhou, C., Keesing, J. K., Serrano, O., Werner, A., Fang, Y., et al. (2022). Wildfires enhance phytoplankton production in tropical oceans. *Nat. Commun.* 13, 1348. doi: 10.1038/s41467-022-29013-0

- Lu, Y., and Deng, S. (2005). Triassic-jurassic sporopollen assemblages on the southern margin of the Junggar basin, Xinjiang and the T-J boundary. *Acta Geol. Sin.* 1, 15–28. doi: 10.3321/j.issn:0001-5717.2005.01.003
- Lu, J., Zhang, P., Dal Corso, J., Yang, M., Wignall, P. B., Greene, S. E., et al. (2021). Volcanically driven lacustrine ecosystem changes during the Carnian Pluvial Episode (Late Triassic). *Proc. Natl. Acad. Sci. U.S.A.* 118, e2109895118. doi: 10.1073/pnas.2109895118
- Lu, J., Zhang, P., Yang, M., Shao, L., and Hilton, J. (2020). Continental records of organic carbon isotopic composition ($\delta^{13}C_{org}$), weathering, paleoclimate and wildfire linked to the End-Permian Mass Extinction. *Chem. Geol.* 558, 119764. doi: 10.1016/j.chemgeo.2020.119764
- Luo, M., Chen, J., Qie, W., Huang, J., Zhang, Q., Zhou, C., et al. (2021). Microbially induced carbonate precipitation in a middle triassic microbial mat deposit from Southwestern China: New implications for the formational process of micrite. *J. Earth Sci.* 32 (3), 633–645. doi: 10.1007/s12583-020-1075-6
- Manfroi, J., Uhl, D., Guerra-Sommer, M., Francischini, H., Martinelli, A. G., Soares, M. B., et al. (2015). Extending the database of Permian palaeo-wildfire on Gondwana: Charcoal remains from the Rio do Rasto Formation (Paraná Basin), Middle Permian, Rio Grande do Sul State, Brazil. *Palaeogeogr. Palaeoclimatol. Palaeoecol.* 436, 77–84. doi: 10.1016/j.palaeo.2015.07.003
- Marynowski, L., and Simoneit, B. R. T. (2009). Widespread upper Triassic to lower Jurassic wildfire records from Poland: Evidence from charcoal and pyrolytic polycyclic aromatic hydrocarbons. *Palaios* 24, 785–798. doi: 10.2110/palo.2009.p09-044r
- Mays, C., McLoughlin, S., Frank, T. D., Fielding, C. R., Slater, S. M., and Vajda, V. (2021). Lethal microbial blooms delayed freshwater ecosystem recovery following the end-Permian extinction. *Nat. Commun.* 12, 5511. doi: 10.1038/s41467-021-25711-3
- Mays, C., Vajda, V., Frank, T. D., Fielding, C. R., Nicoll, R. S., Tevyaw, A. P., et al. (2020). Refined Permian–Triassic floristic timeline reveals early collapse and delayed recovery of south polar terrestrial ecosystems. *GSA Bull.* 132, 1489–1513. doi: 10.1130/B35355.1
- McElwain, J. C., Beerling, D. J., and Woodward, F. I. (1999). Fossil plants and global warming at the Triassic–Jurassic boundary. *Science* 285, 1386–1390. doi: 10.1126/science.285.5432.1386
- McLoughlin, S., Nicoll, R. S., Crowley, J. L., Vajda, V., Mays, C., Fielding, C. R., et al. (2021). Age and paleoenvironmental significance of the frazer beach member—A new lithostratigraphic unit overlying the end-permian extinction horizon in the Sydney basin, Australia. *Front. Earth Sci.* 8. doi: 10.3389/feart.2020.600976
- Miller, C. S., and Baranyi, V. (2021). “Triassic climates,” in *Encyclopedia of Geology*. Eds. D. Alderton and S. A. B. T. Elias (Oxford: Elsevier), 514–524. doi: 10.1016/B978-0-12-409548-9.12070-6
- Murthy, S., Mendhe, V. A., Kavali, P. S., and Singh, V. P. (2020). Evidence of recurrent wildfire from the Permian coal deposits of India: Petrographic, scanning electron microscopic and palynological analyses of fossil charcoal. *Palaeoworld* 29, 715–728. doi: 10.1016/j.palwor.2020.03.004
- Nabbefeld, B., Grice, K., Summons, R. E., Hays, L. E., and Cao, C. (2010). Significance of polycyclic aromatic hydrocarbons (PAHs) in Permian/Triassic boundary sections. *Appl. Geochemistry* 25, 1374–1382. doi: 10.1016/j.apgeochem.2010.06.008
- Nowak, H., Schneebeli-Hermann, E., and Kustatscher, E. (2019). No mass extinction for land plants at the Permian–Triassic transition. *Nat. Commun.* 10, 384. doi: 10.1038/s41467-018-07945-w
- Olsen, P. E., Kent, D. V., Sues, H. D., Koeberl, C., Huber, H., Montanari, A., et al. (2002). Ascent of dinosaurs linked to an iridium anomaly at the Triassic–Jurassic boundary. *Science* 296, 1305–1307. doi: 10.1126/science.1065522
- Petersen, H. I., and Lindström, S. (2012). Synchronous wildfire activity rise and mire deforestation at the triassic–jurassic boundary. *PLoS One* 7, e47236. doi: 10.1371/journal.pone.0047236
- Pieńkowski, G., Niedzwiedzki, G., and Waksmundzka, M. (2012). Sedimentological, palynological and geochemical studies of the terrestrial Triassic–Jurassic boundary in northwestern Poland. *Geol. Mag.* 149, 308–332. doi: 10.1017/S0016756811000914
- Pole, M., Wang, Y., Dong, C., Xie, X., Tian, N., Li, L., et al. (2018). Fires and storms—a Triassic–Jurassic transition section in the Sichuan Basin, China. *Palaeobiodiversity Palaeoenvironments* 98, 29–47. doi: 10.1007/s12549-017-0315-y
- Ruhl, M., Hesselbo, S. P., Al-Suwaidi, A., Jenkyns, H. C., Damborenea, S. E., Manceñido, M. O., et al. (2020). On the onset of Central Atlantic Magmatic Province (CAMP) volcanism and environmental and carbon-cycle change at the Triassic–Jurassic transition (Neuquén Basin, Argentina). *Earth-Science Rev.* 208, 103229. doi: 10.1016/j.earscirev.2020.103229
- Schaller, M. F., Wright, J. D., and Kent, D. V. (2011). Atmospheric PCO₂ perturbations associated with the central atlantic magmatic province. *Science* 331, 1404–1409. doi: 10.1126/science.1199011
- Schneebeli-Hermann, E., Hochuli, P. A., and Bucher, H. (2017). Palynofloral associations before and after the Permian–Triassic mass extinction, Kap Stosch, East Greenland. *Glob. Planet. Change* 155, 178–195. doi: 10.1016/j.gloplacha.2017.06.009
- Scott, A. C. (2000). The Pre-Quaternary history of fire. *Palaeogeogr. Palaeoclimatol. Palaeoecol.* 164, 281–329. doi: 10.1016/S0031-0182(00)00192-9
- Shao, L., Hua, F., Wang, J., Ji, X., Yan, Z., Zhang, T., et al. (2023). Palynological dynamics in the late Permian and the Permian–Triassic transition in southwestern China. *Palaeogeogr. Palaeoclimatol. Palaeoecol.* 619, 111540. doi: 10.1016/j.palaeo.2023.111540
- Sharif, E. (2022). The role of wildfires in a sustainable future. *J. Futur. Sustain.* 2, 17–22. doi: 10.5267/j.jfs.2022.8.003
- Shen, J., Chen, J., Yu, J., Algeo, T. J., Smith, R. M. H., Botha, J., et al. (2023). Mercury evidence from southern Pangea terrestrial sections for end-Permian global volcanic effects. *Nat. Commun.* 14, 6. doi: 10.1038/s41467-022-35272-8
- Shen, S. Z., Crowley, J. L., Wang, Y., Bowring, S. A., Erwin, D. H., Sadler, P. M., et al. (2011). Calibrating the end-Permian mass extinction. *Science* 334, 1367–1372. doi: 10.1126/science.1213454
- Shen, J., Yin, R., Algeo, T. J., Svensen, H. H., and Schoepfer, S. D. (2022a). Mercury evidence for combustion of organic-rich sediments during the end-Triassic crisis. *Nat. Commun.* 13, 1307. doi: 10.1038/s41467-022-28891-8
- Shen, J., Yin, R., Zhang, S., Algeo, T. J., Bottjer, D. J., Yu, J., et al. (2022b). Intensified continental chemical weathering and carbon-cycle perturbations linked to volcanism during the Triassic–Jurassic transition. *Nat. Commun.* 13, 299. doi: 10.1038/s41467-022-27965-x
- Shen, J., Yu, J., Chen, J., Algeo, T. J., Xu, G., Feng, Q., et al. (2019). Mercury evidence of intense volcanic effects on land during the Permian–Triassic transition. *Geology* 47, 1117–1121. doi: 10.1130/G46679.1
- Shu, W., Tong, J., Yu, J., Hilton, J., Benton, M. J., Shi, X., et al. (2022). Permian–Middle Triassic floral succession in North China and implications for the great transition of continental ecosystems. *GSA Bull.* 135, 1747–1767. doi: 10.1130/B36316.1
- Song, Y., Algeo, T. J., Wu, W., Luo, G., Li, L., Wang, Y., et al. (2020). Distribution of pyrolytic PAHs across the Triassic–Jurassic boundary in the Sichuan Basin, southwestern China: Evidence of wildfire outside the Central Atlantic Magmatic Province. *Earth-Science Rev.* 201, 102970. doi: 10.1016/j.earscirev.2019.102970
- Song, Y., Tian, Y., Yu, J., Algeo, T. J., Luo, G., Chu, D., et al. (2022). Wildfire response to rapid climate change during the Permian–Triassic biotic crisis. *Glob. Planet. Change* 215, 103872. doi: 10.1016/j.gloplacha.2022.103872
- Sun, Y., Joachimski, M. M., Wignall, P. B., Yan, C., Chen, Y., Jiang, H., et al. (2012). Lethally hot temperatures during the early triassic greenhouse. *Science* 338, 366–370. doi: 10.1126/science.1224126
- Vajda, V., Calner, M., and Ahlberg, A. (2013). Palynostratigraphy of dinosaur footprint-bearing deposits from the Triassic–Jurassic boundary interval of Sweden. *GFF* 135, 120–130. doi: 10.1080/11035897.2013.799223
- Vajda, V., McLoughlin, S., Mays, C., Frank, T. D., Fielding, C. R., Tevyaw, A., et al. (2020). End-Permian (252 Mya) deforestation, wildfires and flooding—An ancient biotic crisis with lessons for the present. *Earth Planet. Sci. Lett.* 529, 115875. doi: 10.1016/j.epsl.2019.115875
- van de Schootbrugge, B., Payne, J. L., Tomasovych, A., Pross, J., Fiebig, J., Benbrahim, M., et al. (2008). Carbon cycle perturbation and stabilization in the wake of the Triassic–Jurassic boundary mass-extinction event. *Geochemistry Geophys. Geosystems* 9, n/a–n/a. doi: 10.1029/2007GC001914
- van de Schootbrugge, B., Quan, T. M., Lindström, S., Püttmann, W., Heunisch, C., Pross, J., et al. (2009). Floral changes across the Triassic/Jurassic boundary linked to flood basalt volcanism. *Nat. Geosci.* 2, 589–594. doi: 10.1038/ngeo577
- van de Schootbrugge, B., van der Weijst, C. M. H., Hollaar, T. P., Vecoli, M., Strother, P. K., Kuhlmann, N., et al. (2020). Catastrophic soil loss associated with end-Triassic deforestation. *Earth-Science Rev.* 210, 103332. doi: 10.1016/j.earscirev.2020.103332
- Wang, Z., and Chen, A. (2001). Traces of arborescent lycopsids and dieback of the forest vegetation in relation to the terminal Permian mass extinction in North China. *Rev. Palaeobot. Palynol.* 117, 217–243. doi: 10.1016/S0034-6667(01)00094-X
- Whiteside, J. H., Olsen, P. E., Kent, D. V., Fowell, S. J., and Et-Touhami, M. (2007). Synchrony between the Central Atlantic magmatic province and the Triassic–Jurassic mass-extinction event? *Palaeogeogr. Palaeoclimatol. Palaeoecol.* 244, 345–367. doi: 10.1016/j.palaeo.2006.06.035
- Wignall, P. B., and Atkinson, J. W. (2020). A two-phase end-Triassic mass extinction. *Earth-Science Rev.* 208, 103282. doi: 10.1016/j.earscirev.2020.103282
- Wu, Y., Chu, D., Tong, J., Song, H. J., Dal Corso, J., Wignall, P. B., et al. (2021). Six-fold increase of atmospheric pCO₂ during the Permian–Triassic mass extinction. *Nat. Commun.* 12, 2137. doi: 10.1038/s41467-021-22298-7
- Wu, Y., Cui, Y., Chu, D., Song, H., Tong, J., Dal Corso, J., et al. (2023). Volcanic CO₂ degassing postdates thermogenic carbon emission during the end-Permian mass extinction. *Sci. Adv.* 9, eabq4082. doi: 10.1126/sciadv.abq4082
- Wu, Y., Tong, J., Algeo, T. J., Chu, D., Cui, Y., Song, H. Y., et al. (2020). Organic carbon isotopes in terrestrial Permian–Triassic boundary sections of North China: Implications for global carbon cycle perturbations. *Bull. Geol. Soc. Am.* 132, 1106–1118. doi: 10.1130/B35228.1
- Xu, X., Shao, L., Eriksson, K. A., Zhou, J., Wang, D., Hou, H., et al. (2022). Widespread wildfires linked to early Albian Ocean Anoxic Event 1b: Evidence from the Fuxin lacustrine basin, NE China. *Glob. Planet. Change* 215, 103858. doi: 10.1016/j.gloplacha.2022.103858
- Yan, Z., Shao, L., Glasspool, I. J., Wang, J., Wang, X., and Wang, H. (2019). Frequent and intense fires in the final coals of the Paleozoic indicate elevated atmospheric oxygen levels at the onset of the End-Permian Mass Extinction Event. *Int. J. Coal Geol.* 207, 75–83. doi: 10.1016/j.coal.2019.03.016

Yang, G. X., and Wang, H. S. (2012). Yuzhou Flora-A hidden gem of the Middle and Late Cathaysian Flora. *Sci. China Earth Sci.* 55, 1601–1619. doi: 10.1007/s11430-012-4476-2

Zhang, H., Cao, C. Q., Liu, X. L., Mu, L., Zheng, Q. F., Liu, F., et al. (2016). The terrestrial end-Permian mass extinction in South China. *Palaeogeogr. Palaeoclimatol. Palaeoecol.* 448, 108–124. doi: 10.1016/j.palaeo.2015.07.002

Zhang, P., Lu, J., Yang, M., Bond, D. P. G., Greene, S. E., Liu, L., et al. (2022). Volcanically-induced environmental and floral changes across the Triassic-Jurassic (T-J) transition. *Front. Ecol. Evol.* 10. doi: 10.3389/fevo.2022.853404

Zhang, P., Yang, M., Lu, J., Bond, D. P. G., Zhou, K., Xu, X., et al. (2023a). End-Permian terrestrial ecosystem collapse in North China: Evidence from palynology and geochemistry. *Glob. Planet. Change* 222, 104070. doi: 10.1016/j.gloplacha.2023.104070

Zhang, P., Yang, M., Lu, J., Jiang, Z., Zhou, K., Xu, X., et al. (2023b). Floral response to the late triassic carnian pluvial episode. *Front. Ecol. Evol.* 11. doi: 10.3389/fevo.2023.1199121

Zhou, N., Xu, Y., Li, L., Lu, N., An, P., Popa, M. E., et al. (2021). Pattern of vegetation turnover during the end-Triassic mass extinction: Trends of fern communities from South China with global context. *Glob. Planet. Change* 205, 103585. doi: 10.1016/j.gloplacha.2021.103585